# Movement decomposition in the primary motor cortex

Naama Kadmon Harpaz[1], David Ungarish[1], Nicholas G. Hatsopoulos[2,3], and Tamar Flash[1]

## SUPPLEMENTARY MATERIAL

[1] Department of Computer Science and Applied Mathematics, Weizmann Institute of Science, Rehovot 7610001, Israel

[2] Committee on Computational Neuroscience, University of Chicago, Chicago, IL 60637, USA

[3] Department of Organismal Biology and Anatomy, University of Chicago, Chicago, IL 60637, USA

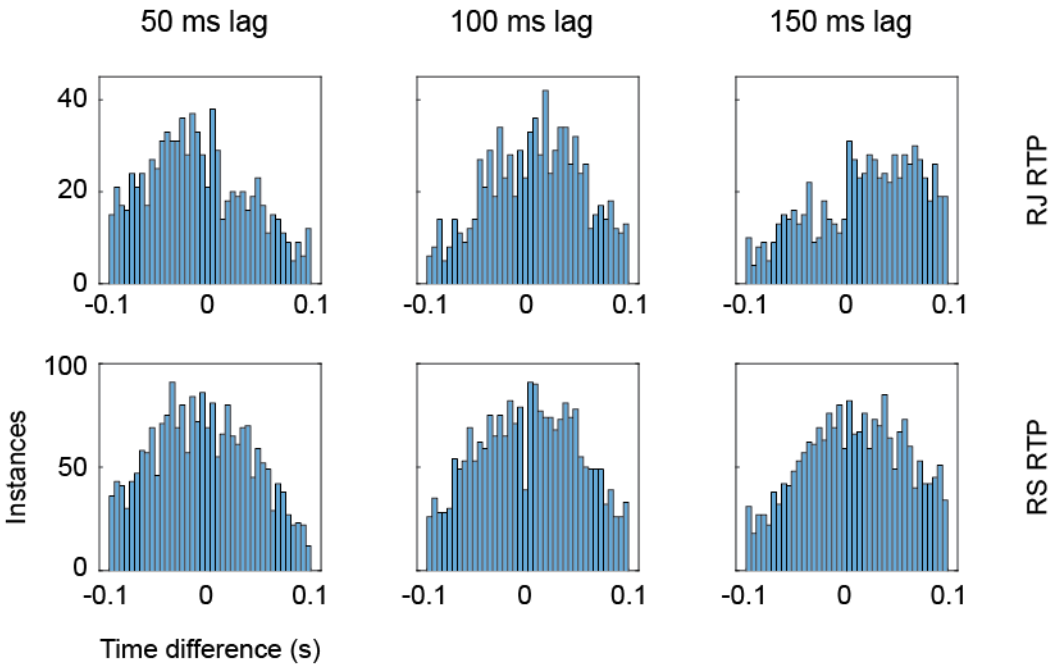


Supplementary figure 1. **Distances between neural state transition points and speed extrema when using different time lags**. Time points of neural state transitions were coupled to time points of speed maxima and minima in the RTP trials using a cost-based metric (see Methods), taking into account a lag of 50 ms (left panels), 100 ms (middle panels), and 150 ms (right panels). The plotted histograms summarize the time differences found between coupled pairs of state transitions and speed extrema. As can be clearly seen for monkey RJ (top panels) and to a lesser extent for monkey RS (bottom panels), a lag of 100 ms resulted in the most symmetrical distribution of distances, centered on zero.

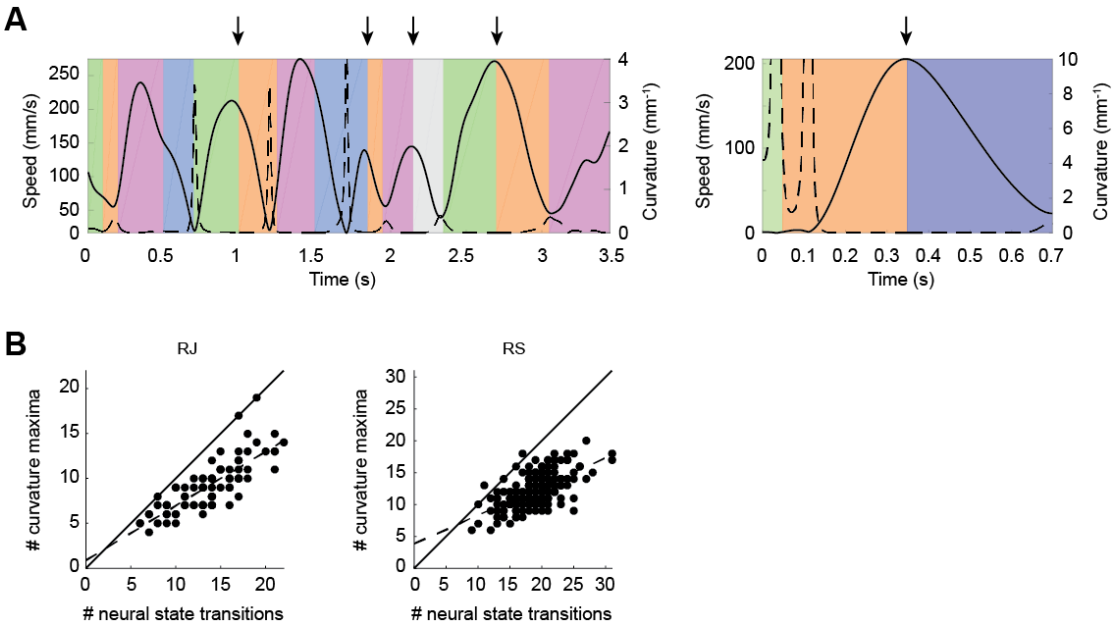


Supplementary figure 2. **Relation of neural segmentation to path curvature**. **A -** Speed (solid line) and curvature (dashed line) profiles of example trials from the RTP task (left, data from RJ) and center-out task (right, data from RS). Background colors denote the decoded neural states. As can be seen in the RTP trial, curvature maxima were coupled to speed minima, and coincided with neural state transitions. However, as indicated by the arrows on top, neural state transitions also coincided with speed maxima points, which occurred during straight path segments. This is also evident in the center-out trial, in which a neural state transition coincides with peak speed, which occurs during a straight movement. **B -** The number of neural state transitions vs. the number of curvature maxima across trials in the RTP task. Each point represents a single trial, dashed line represents the linear regression line, and solid line represents the 45º line. Left panel - RJ, right panel - RS. The scatter plots show that the number of neural state transitions consistently exceeded the number of curvature maxima within a trial.

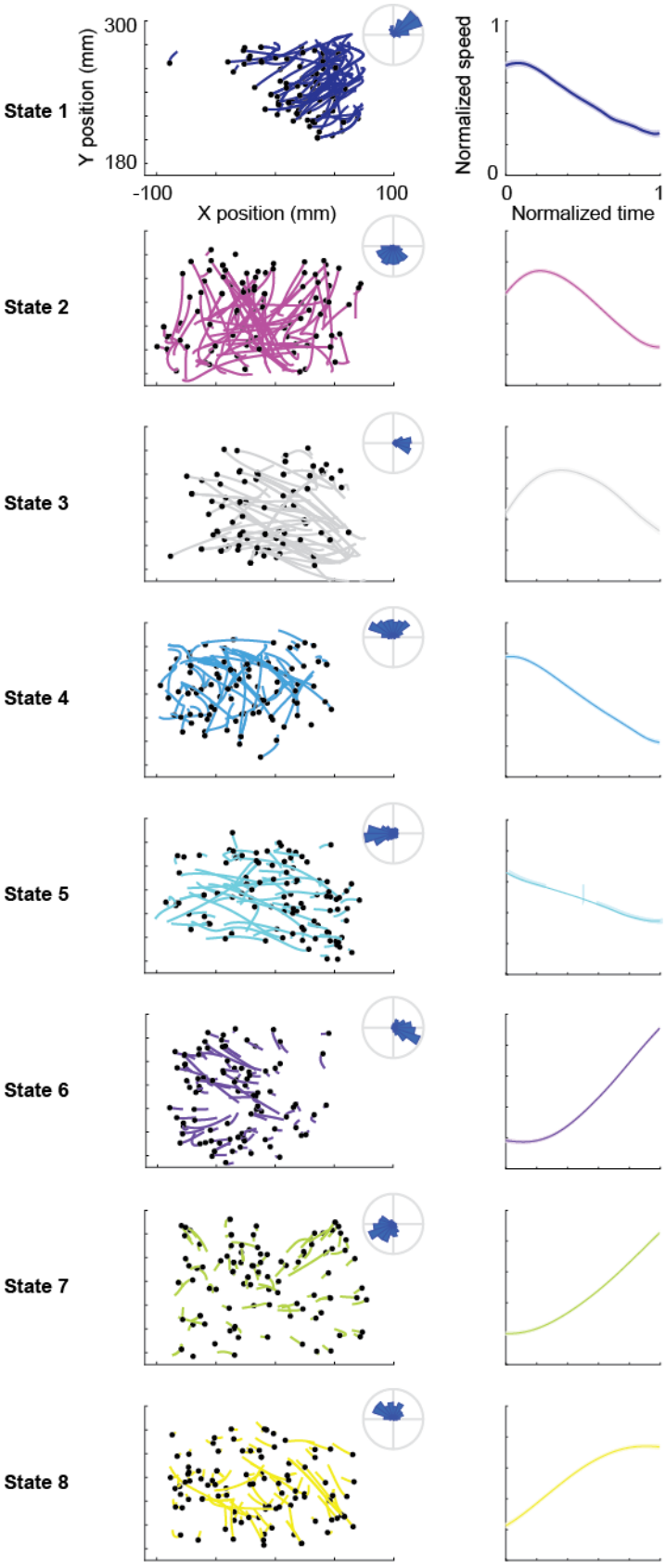


Supplementary Figure 3. **Directional and acceleration selectivity across trials**. **Left -** Each panel shows movement segments corresponding to a specific neural state. Each line is a single segment, black dots represent the beginning of the segment. For visualization purposes we only show a random subset of the segments. Radial histograms show the distribution of directions within each state. **Right -** Each panel shows the mean ± sem of the normalized speed profiles of movement segments corresponding to a single neural state. Data from RS.

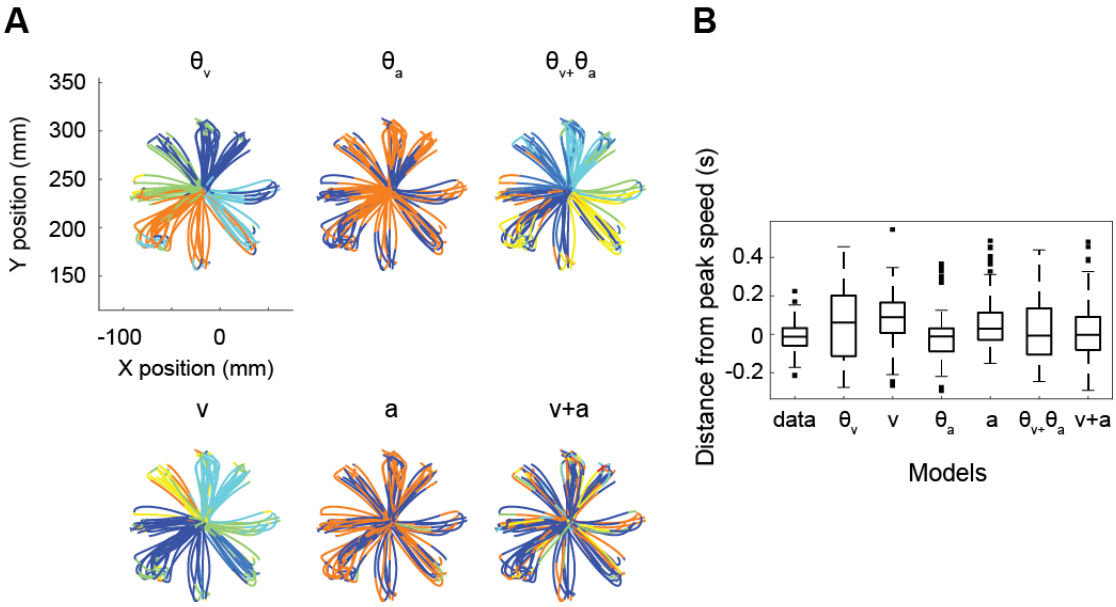


Supplementary Figure 4. **Movement segmentation according to simulated neural populations in the center-out task**. Simulated firing rates according to six different instantaneous kinematic models were used for HMM training and decoding (see Methods). The models included tuning for: movement direction ($\theta_v$); movement direction gain modulated by speed ($v$); direction of the acceleration vector ($\theta_a$); direction of the acceleration vector gain modulated by the magnitude of the acceleration vector ($a$); both movement direction and direction of the acceleration vector ($\theta_v + \theta_a$); or both movement direction and direction of the acceleration vector, each gain modulated by the magnitude of the corresponding vector ($v + a$), and were formulated according to all or parts of -

$$fr_i(t-\tau) = B_{0_i} + B_{1_i}\|\vec{v}(t)\|\cos\left(\theta_v(t) - \theta_{v\,pd_i}\right) + B_{2_i}\|\vec{a}(t)\|\cos\left(\theta_a(t) - \theta_{apd_i}\right)$$

(see Methods for further details). **A -** Position data from the decoded center-out trials colored according to the identified neural states obtained from the six simulated models. Compare to **Figure 5B**. **B -** Box plots of the distances between peak speed and the nearest neural transition point, with the distribution for the actual data on the left and for the simulated models subsequently on the right, showing that the actual distances were lower compared to the distances found in the simulated data. Results shown are from models trained on 7 states (such that it will be comparable to the results shown for the actual data), using the training iteration that produced the lowest average absolute distance between peak speed and the nearest neural transition in the test trials. Similar results were found when using 4-10 states as well (results not shown).

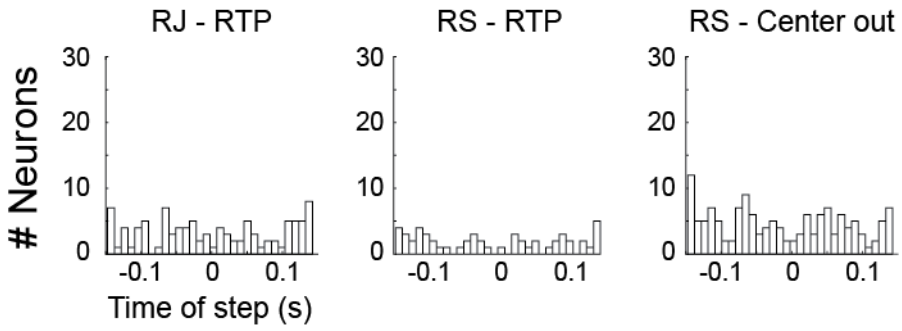


Supplementary Figure 5. **Modulation in the activity of single cells using random transition points**. Random transition points were generated for each trial according to the distribution of neural state durations obtained from the original model. These random transitions were then used similarly to the original transitions, as described in *Single cell activation and correspondence to neural states* in the Methods section. I.e., mean firing patterns for each neuron per state-pair were calculated after aligning the extracted 300 ms time windows around random transition points. We repeated this analysis by generating 50 sets of random transitions per dataset. As expected, this resulted in noisy mean firing rates, which were poorly fitted by regression trees (mean ± SD $R^2$ = 0.28±0.08, 0.34±0.09, 0.4±0.13, correspondingly for RJ RTP, RS RTP, and RS Center-out datasets). Histograms of the time of the step of the best fitted regression trees showed no evident peak, as demonstrated for a single iteration of each dataset in the figure above. We calculated the percentage of cells which step occurred less than 10 ms around the point of transition per iteration. This yielded null distributions with mean values equal to 4%±2% SD, 6%±2%, and 6%±2%, correspondingly for RJ RTP, RS RTP, and RS Center-out datasets. The percentiles obtained from the actual model were significantly higher compared to these null distributions ($P < 0.001$, for all datasets).

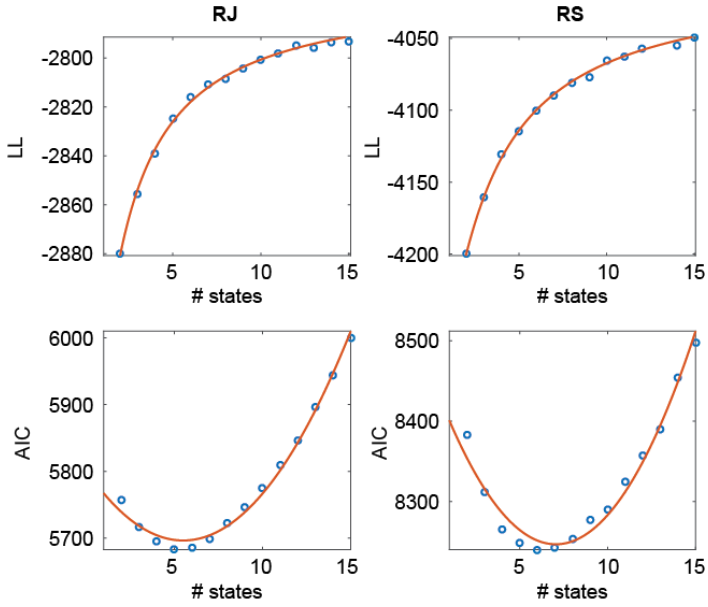


Supplementary Figure 6. **Graphs of the log likelihood (top) and the AIC (bottom) of the model, versus number of hidden states, estimated on the test set**. The log likelihood reached a plateau starting around 5-6 for RJ and around 7-8 for RS. The AIC reached minimum around a similar number of states.